

## A NINE POINT SCHEME FOR THE APPROXIMATION OF DIFFUSION OPERATORS ON DISTORTED QUADRILATERAL MESHES\*

ZHIQIANG SHENG<sup>†</sup> AND GUANGWEI YUAN<sup>†</sup>

**Abstract.** A nine point scheme is presented for discretizing diffusion operators on distorted quadrilateral meshes. The advantage of this method is that highly distorted meshes can be used without the numerical results being altered remarkably, and it treats material discontinuities rigorously and offers an explicit expression for the face-centered flux; moreover, it has only the cell-centered unknowns. We prove that the method is stable and has first-order convergence on distorted meshes. Numerical experiments show that the method has second-order or nearly second-order accuracy on distorted meshes.

**Key words.** finite volume scheme, nine point scheme, diffusion equation, distorted meshes, convergence

**AMS subject classifications.** 65M06, 65M12, 65M55

**DOI.** 10.1137/060665853

**1. Introduction.** Accurate and reliable discretization methods for the diffusion equation on distorted meshes are very important for numerical simulations of Lagrangian hydrodynamics and magnetohydrodynamics. As with the finite element method and the finite difference method, the finite volume method is a discretization technique for solving partial differential equations (PDEs). It is obtained by integrating the PDEs over a control volume, and it represents in general the conservation of certain physical quantities of interest, such as mass, momentum, or energy. Due to this natural association, the finite volume method is widely used in practical problems such as computational fluid dynamics [18]. Moreover, it is flexible enough to be applied to complex space domains, and because it works directly on the physical domain rather than on the computational domain through coordinate transformations, it can be easily used in adaptive mesh strategies.

A finite volume scheme for solving diffusion equations on nonrectangular meshes is proposed in [10], which is the so-called nine point scheme on arbitrary quadrilateral meshes. This scheme has only cell-centered unknowns after cell-vertex unknowns are eliminated by taking them as the arithmetic average of the neighboring cell-centered unknowns. However, this simple interpolation loses significant accuracy on moderately and highly skewed meshes. Some similar schemes are discussed in [8, 17].

The scheme in [7] has both cell-centered unknowns and vertex unknowns and leads to a symmetric positive definite matrix. Although numerical experiments show that this scheme indeed has second-order accuracy, no theoretical proof is given. In [19], the authors analyze the scheme theoretically, and give a construction of a finite volume scheme for diffusion equations with discontinuous coefficients. The theoretical

---

\*Received by the editors July 24, 2006; accepted for publication (in revised form) December 4, 2007; published electronically March 21, 2008. This work was partially supported by the National Basic Research Program (2005CB321703), the National Nature Science Foundation of China (60533020), and Basic Research Project of National Defense (A1520070074).

<http://www.siam.org/journals/sisc/30-3/66585.html>

<sup>†</sup>Laboratory of Computational Physics, Institute of Applied Physics and Computational Mathematics, P.O. Box 8009, Beijing, 100088, China (szqdx@163.com, yuan.guangwei@iapcm.ac.cn).

analysis of the scheme is also given in [6]; moreover, the method is extended to Leray–Lions-type elliptic problems in [5].

The scheme in [9] consists of a cell-centered variational method based on a smooth mapping between the logical mesh coordinates and the spatial coordinates. This scheme leads to a symmetric positive definite matrix. However, the assumption of a smooth mapping is too restrictive. It also loses significant accuracy on moderately and highly skewed meshes.

The MDHW scheme in [12] rigorously treats material discontinuities and yields second-order accuracy regardless of the smoothness of the mesh. This scheme has face-centered unknowns in addition to cell-centered unknowns. The support operators method (SOM) in [11, 13, 15, 16] gives second-order accuracy on both smooth and nonsmooth meshes either with or without material discontinuities, and SOM generally leads to a symmetric positive definite matrix. However, SOM has both cell-centered and face-centered unknowns or has a dense diffusion matrix, and there is no explicit discrete expression for the normal flux on a cell edge.

The method of multipoint flux approximations (MPFA) [1, 2, 3, 4] has only cell-centered unknowns and gives an explicit expression for the face-centered flux. The flux is approximated by a multipoint flux expression based on transmissibility coefficients. These coefficients are computed by locally solving a small linear system.

In this paper we present a nine point scheme for diffusion equations with continuous and discontinuous coefficients on distorted quadrilateral meshes. The basic idea for constructing the scheme is as follows. First, by integrating the diffusion equation over a control volume (cell) and using the Gauss theorem, we obtain the expression for the integral flux on a cell side. Second, we discretize the flux using cell-centered unknowns, vertex unknowns, and face-centered unknowns on each cell. Third, we eliminate the face-centered unknowns by continuity of the normal flux component across a cell edge. Then we eliminate the vertex unknowns using the cell-centered unknowns, and the elimination procedure is a focus of this work. Hence, there are only cell-centered unknowns in the expression of our discrete normal flux. Furthermore, it is worth pointing out that the expression for the normal flux component has a specific physical meaning and an intuitive geometric explanation, so it facilitates implementation in codes. In addition, we can obtain the vertex values, which are important in some numerical methods of Lagrangian magnetohydrodynamics. Our scheme reduces to the standard five point scheme on rectangular grids and often leads to a nonsymmetric matrix for general quadrilateral meshes. We prove that our scheme is stable and gives first-order convergence. Moreover, we extend the method to general model diffusion problems. Although we prove only that the scheme is first-order accurate, the numerical experiments show that it is nearly second-order accurate on distorted meshes.

The rest of this paper is organized as follows. In section 2, we describe the construction of the finite volume scheme for stationary diffusion problems on distorted quadrilateral meshes. In section 3, we prove that the scheme is stable and has first-order accuracy. We extend the method to general model diffusion problems in section 4. Then we present some numerical experiments to show their performance on several test problems in section 5. Finally, we end with some concluding remarks.

## 2. Construction of scheme for diffusion equation.

**2.1. Problem and notation.** Consider the stationary diffusion problem

$$(2.1) \quad -\nabla \cdot (\kappa(x)\nabla u) = f(x) \quad \text{in } \Omega,$$

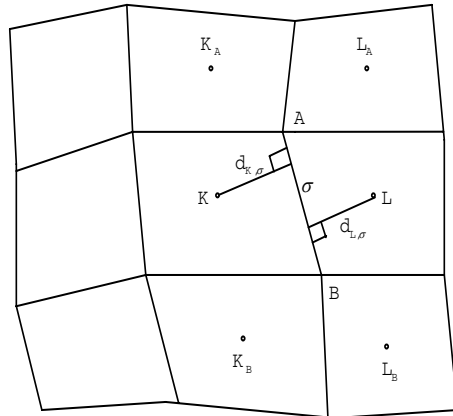


FIG. 2.1. The mesh stencil.

$$(2.2) \quad u(x) = 0 \quad \text{on } \partial\Omega,$$

where  $\Omega$  is an open bounded polygonal set of  $R^2$  with boundary  $\partial\Omega$ .

Let us denote the cell and cell center by  $K$  and  $L$ , the vertex by  $A$  and  $B$ , and the cell side by  $\sigma$  (see Figure 2.1). If the cell side  $\sigma$  is a common edge of cells  $K$  and  $L$ , and its vertices are  $A$  and  $B$ , then we denote

$$\sigma = K|L = BA.$$

Let  $\mathcal{J}$  be the set of all cells,  $\mathcal{E}$  be the set of all cell sides,  $\mathcal{E}_{int}$  be the set of all cell sides not on  $\partial\Omega$ ,  $\mathcal{E}_{ext}$  be the set of all cell sides on  $\partial\Omega$ , and  $\mathcal{E}_K$  be the set of all cell sides of cell  $K$ . Denote  $h = (\sup_{K \in \mathcal{J}} m(K))^{1/2}$ , where  $m(K)$  is the area of cell  $K$ .

We need the following two assumptions.

Assumption (H1):  $u(x) \in C^2(K)$ ,  $\kappa(x) \in C^1(K)$ , and  $f(x) \in C^1(K)$  for all  $K \in \mathcal{J}$ .

Assumption (H2): There is a constant  $C > 0$  such that

$$\frac{1}{C}|A - B| \leq |K - L| \leq C|A - B|, \quad K \in \mathcal{J}.$$

Assumption (H2) implies that the aspect ratio is bounded; i.e., there are no extremely long and thin cells.

**2.2. The expression of flux.** By integrating (2.1) over the cell  $K$  and using the Green formula, one obtains

$$(2.3) \quad \sum_{\sigma \in \mathcal{E}_K} \mathcal{F}_{K,\sigma} = \int_K f(x) dx,$$

where  $\mathcal{F}_{K,\sigma}$  is the normal face flux on the edge  $\sigma$ , defined by

$$(2.4) \quad \mathcal{F}_{K,\sigma} = - \int_{\sigma} \kappa(x) \nabla u(x) \cdot \vec{n}_{K,\sigma} dl,$$

with  $\vec{n}_{K,\sigma}$  the outward unit normal on the edge  $\sigma$  of cell  $K$  (see Figure 2.2).

In Figure 2.2,  $I$  is the midpoint of  $\sigma = BA$ ;  $\vec{\tau}_{BA}$  and  $\vec{\tau}_{KI}$  are unit tangential vectors on  $BA$  and  $KI$ , respectively; and  $\theta_{K,\sigma}$  is the angle between  $\vec{n}_{K,\sigma}$  and  $\vec{\tau}_{KI}$ . Notice that

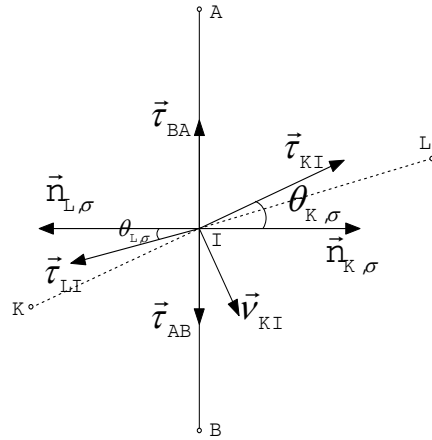


FIG. 2.2. Some notation.

$$\vec{n}_{K,\sigma} = -\tan \theta_{K,\sigma} \vec{\tau}_{BA} + \frac{1}{\cos \theta_{K,\sigma}} \vec{\tau}_{KI},$$

and the normal face flux can be written as

$$(2.5) \quad \mathcal{F}_{K,\sigma} = \tan \theta_{K,\sigma} \int_{\sigma} \kappa(x) \nabla u(x) \cdot \vec{\tau}_{BA} dl - \frac{1}{\cos \theta_{K,\sigma}} \int_{\sigma} \kappa(x) \nabla u(x) \cdot \vec{\tau}_{KI} dl.$$

By the Taylor expansion, one has

$$u(I) - u(K) = \nabla u(x) \cdot (I - K) + \frac{1}{2}(H_I - H_K),$$

$$u(A) - u(B) = \nabla u(x) \cdot (A - B) + \frac{1}{2}(H_A - H_B),$$

where  $H_I = (\nabla^2 u(rx + (1-r)I)(I-x), I-x)$ ,  $\nabla^2 u(rx + (1-r)I)$  is the Hessian matrix of  $u$  at the point  $rx + (1-r)I$ , and  $r$  is a number in  $[0, 1]$ . The other notations  $H_K$ ,  $H_A$ , and  $H_B$  have similar meanings. It follows that

$$\begin{aligned} \kappa(x) \nabla u(x) \cdot \vec{\tau}_{KI} &= \frac{\kappa(K)}{|I-K|} (u(I) - u(K)) - \kappa(K) \frac{H_I - H_K}{2|I-K|} \\ &\quad - (\nabla \kappa(rx + (1-r)x) \cdot (K-x)) \nabla u(x) \cdot \vec{\tau}_{KI}, \\ \kappa(x) \nabla u(x) \cdot \vec{\tau}_{BA} &= \frac{\kappa(K)}{|A-B|} (u(A) - u(B)) - \kappa(K) \frac{H_A - H_B}{2|A-B|} \\ &\quad - (\nabla \kappa(rx + (1-r)x) \cdot (K-x)) \nabla u(x) \cdot \vec{\tau}_{BA}. \end{aligned}$$

Substitute the above two equations into (2.5) to obtain

$$(2.6) \quad \mathcal{F}_{K,\sigma} = -\tau_{K,\sigma} (u(I) - u(K) - D_{K,\sigma}(u(A) - u(B))) + R_{K,\sigma},$$

where  $\tau_{K,\sigma} = \frac{|A-B|\kappa(K)}{|I-K|\cos\theta_{K,\sigma}} = \frac{|A-B|\kappa(K)}{d_{K,\sigma}}$ ,  $D_{K,\sigma} = \frac{\sin\theta_{K,\sigma}|I-K|}{|A-B|}$ , and  $R_{K,\sigma} = O(h^2)$ . Similarly, we have

$$(2.7) \quad \mathcal{F}_{L,\sigma} = -\tau_{L,\sigma}(u(I) - u(L) - D_{L,\sigma}(u(B) - u(A))) + R_{L,\sigma},$$

where  $\tau_{L,\sigma} = \frac{|A-B|\kappa(L)}{|I-L|\cos\theta_{L,\sigma}} = \frac{|A-B|\kappa(L)}{d_{L,\sigma}}$ ,  $D_{L,\sigma} = \frac{\sin\theta_{L,\sigma}|I-L|}{|A-B|}$ , and  $R_{L,\sigma} = O(h^2)$ .

By continuity of the normal flux component

$$(2.8) \quad \mathcal{F}_{K,\sigma} = -\mathcal{F}_{L,\sigma},$$

we can obtain

$$(2.9) \quad u(I) = \frac{1}{\tau_{K,\sigma} + \tau_{L,\sigma}}(\tau_{K,\sigma}u(K) + \tau_{L,\sigma}u(L) + (\tau_{K,\sigma}D_{K,\sigma} - \tau_{L,\sigma}D_{L,\sigma})(u(A) - u(B))) + \frac{1}{\tau_{K,\sigma} + \tau_{L,\sigma}}(R_{K,\sigma} + R_{L,\sigma}).$$

Substitute (2.9) into (2.6) to obtain

$$(2.10) \quad \mathcal{F}_{K,\sigma} = -\tau_\sigma(u(L) - u(K) - D_\sigma(u(A) - u(B))) + \bar{R}_{K,\sigma},$$

where  $\tau_\sigma = \frac{\tau_{K,\sigma}\tau_{L,\sigma}}{\tau_{K,\sigma} + \tau_{L,\sigma}} = \frac{|A-B|}{\frac{d_{K,\sigma}}{\kappa(K)} + \frac{d_{L,\sigma}}{\kappa(L)}}$ ,  $D_\sigma = \frac{(L-K, A-B)}{|A-B|^2}$ , and  $\bar{R}_{K,\sigma} = \frac{\tau_{L,\sigma}R_{K,\sigma} - \tau_{K,\sigma}R_{L,\sigma}}{\tau_{K,\sigma} + \tau_{L,\sigma}} = O(h^2)$ . By (2.8) and (2.10), we immediately get

$$(2.11) \quad \mathcal{F}_{L,\sigma} = -\tau_\sigma(u(K) - u(L) - D_\sigma(u(B) - u(A))) + \bar{R}_{L,\sigma},$$

where  $\bar{R}_{L,\sigma} = -\bar{R}_{K,\sigma}$ .

The expressions for the normal flux components have specific physical meanings and clear geometric meanings. For instance,  $\mathcal{F}_{K,\sigma}$  consists of two parts: one is the flux from the cell center  $K$  to the cell center  $L$ , and the other is the flux from the vertex  $B$  to the vertex  $A$ . If the lines  $KL$  and  $AB$  are perpendicular with each other, then the normal flux component  $\mathcal{F}_{K,\sigma}$  is equal to the flux from the cell center  $K$  to the cell center  $L$ , and the flux from the vertex  $B$  to the vertex  $A$  has no contribution for  $\mathcal{F}_{K,\sigma}$ . If the lines  $KL$  and  $AB$  are not perpendicular with each other, then both the flux from the cell center  $K$  to the cell center  $L$  and the flux from the vertex  $B$  to the vertex  $A$  have contribution for  $\mathcal{F}_{K,\sigma}$ .

It is obvious that there are vertex unknowns  $u(A)$  and  $u(B)$  in addition to cell-centered unknowns in the expressions (2.10) and (2.11) of the normal flux component. In the next section, we will consider how to eliminate the vertex unknowns.

**2.3. The expression of vertex unknowns.** The main goal of this section is to obtain the local expression of the normal flux component with only cell-centered unknowns. We will propose a method of eliminating the vertex unknowns in (2.10) and (2.11) by locally approximating them with surrounding cell-centered unknowns. Noticing that  $\bar{R}_{K,\sigma} = O(h^2)$  in (2.10) and  $\bar{R}_{L,\sigma} = O(h^2)$  in (2.11), we require that the approximation of vertex unknowns be second order so as not to affect the approximate accuracy of the normal flux. Now, we will describe in detail a method of eliminating the vertex unknowns.

**2.3.1. Continuous coefficient.** Let  $K_A, L_A, K$ , and  $L$  be the cells sharing the vertex  $A$ . When the coefficient  $\kappa(x)$  is continuous, we use the following Taylor expansions:

$$\begin{aligned} u(K_A) &= u(A) + u_x x_{K_A A} + u_y y_{K_A A} + O(h^2), \\ u(K) &= u(A) + u_x x_{K A} + u_y y_{K A} + O(h^2), \\ u(L) &= u(A) + u_x x_{L A} + u_y y_{L A} + O(h^2), \\ u(L_A) &= u(A) + u_x x_{L_A A} + u_y y_{L_A A} + O(h^2), \end{aligned}$$

where  $x_{K_A A} = x_{K_A} - x_A$ ,  $y_{K_A A} = y_{K_A} - y_A$ , and the others have similar definitions.

As referred to above, we will approximate  $u(A)$  by the linear weighted combination of  $u(K_A), u(L_A), u(K)$ , and  $u(L)$ . In order to make this approximation second order, we should select some coefficients such that the terms containing  $u_x$  and  $u_y$  vanish. Specifically, multiply the above four equations by  $\omega_{A_i}$  ( $i = 1, 2, 3, 4$ ), respectively, and add the resulting equations to obtain

$$(2.12) \quad u(A) = \omega_{A_1} u(K_A) + \omega_{A_2} u(K) + \omega_{A_3} u(L) + \omega_{A_4} u(L_A) + R_A,$$

where  $\omega_{A_i}$  ( $i = 1, 2, 3, 4$ ) satisfy the following relation:

$$(2.13) \quad \begin{cases} \omega_{A_1} + \omega_{A_2} + \omega_{A_3} + \omega_{A_4} = 1, \\ x_{K_A A} \omega_{A_1} + x_{K A} \omega_{A_2} + x_{L A} \omega_{A_3} + x_{L_A A} \omega_{A_4} = 0, \\ y_{K_A A} \omega_{A_1} + y_{K A} \omega_{A_2} + y_{L A} \omega_{A_3} + y_{L_A A} \omega_{A_4} = 0, \end{cases}$$

and  $R_A = O(h^2)$ .

The matrix associated with the system of equations (2.13) is denoted by  $M$ , which is of size  $3 \times 4$ . Thus the linear system (2.13) reduces to an underdetermined system  $M\omega = b$ , where  $\omega = (\omega_{A_1}, \omega_{A_2}, \omega_{A_3}, \omega_{A_4})^T$  and  $b = (1, 0, 0)^T$ . We can obtain the solution  $\omega$  by different methods. In this paper, we set  $\omega = M^T \omega'$  and solve the system of equations about  $\omega'$ :  $MM^T \omega' = b$ . Since the meshes are convex quadrangles, the four points  $K_A, K, L_A$ , and  $L$  are not on a straight line. It follows that the determinant of  $MM^T$  is not equal to zero. Once the solution  $\omega'$  is computed, the original unknown  $\omega$  can be obtained (see [14]).

In a similar way, we have

$$(2.14) \quad u(B) = \omega_{B_1} u(K) + \omega_{B_2} u(K_B) + \omega_{B_3} u(L_B) + \omega_{B_4} u(L) + R_B,$$

where  $\omega_{B_i}$  ( $i = 1, 2, 3, 4$ ) are required to satisfy a similar relation and  $R_B = O(h^2)$ .

**2.3.2. Discontinuous coefficient.** When the diffusion coefficient  $\kappa(x)$  is discontinuous (piecewise continuous), the gradient of  $u(x)$  is discontinuous across the discontinuity. That is,  $u_x$  and  $u_y$  in the Taylor expansion formulae of the above subsection may be discontinuous across the discontinuity. In this case, we use the continuity of the normal flux components at a vertex and the continuity of the tangential gradients on a cell side to eliminate the vertex unknowns. Next, we present the elimination procedure in detail.

We use the following Taylor expansions:

$$(2.15) \quad u(K_A) = u(A) + \nabla u(A)|_{K_A} \cdot (x_{K_A} - x_A) + \bar{R}_{K_A},$$

$$(2.16) \quad u(K) = u(A) + \nabla u(A)|_K \cdot (x_K - x_A) + \bar{R}_K,$$

$$(2.17) \quad u(L) = u(A) + \nabla u(A)|_L \cdot (x_L - x_A) + \bar{R}_L,$$

$$(2.18) \quad u(L_A) = u(A) + \nabla u(A)|_{L_A} \cdot (x_{L_A} - x_A) + \bar{R}_{L_A},$$

where  $\nabla u(A)|_{K_A}$  is the gradient of  $u(x)$  on cell  $K_A$  taking the value at the vertex  $A$ , and  $\nabla u(A)|_K$ ,  $\nabla u(A)|_L$ , and  $\nabla u(A)|_{L_A}$  have similar meanings. Moreover,  $\bar{R}_{K_A} = O(h^2)$ ,  $\bar{R}_K = O(h^2)$ ,  $\bar{R}_{L_A} = O(h^2)$ , and  $\bar{R}_L = O(h^2)$ .

To approximate  $u(A)$  by the linear combination of  $u(K_A)$ ,  $u(K)$ ,  $u(L)$ , and  $u(L_A)$  with second-order accuracy, we choose the combination coefficients such that the terms containing  $\nabla u(A)|_{K_A}$ ,  $\nabla u(A)|_K$ ,  $\nabla u(A)|_L$ , and  $\nabla u(A)|_{L_A}$  vanish. This can be done by using the continuity of the normal flux component at a vertex and the continuity of the tangential gradients on a cell side.

The normal fluxes at vertex  $A$  on the sides  $S_1$ ,  $S_2$ ,  $S_3$ , and  $S_4$  are denoted by  $f_1$ ,  $f_2$ ,  $f_3$ , and  $f_4$ , respectively, where counterclockwise is taken to be the positive flux direction (see Figure 2.3). By the continuity of the normal flux components at vertex  $A$  for each edge, we have

$$(2.19) \quad \kappa(K_A)\nabla u(A)|_{K_A} \cdot \bar{n}_{K_A K} + \bar{R}_1 = -\kappa(K)\nabla u(A)|_K \cdot \bar{n}_{K K_A} + \bar{R}_2 \equiv f_1,$$

$$(2.20) \quad \kappa(K)\nabla u(A)|_K \cdot \bar{n}_{K L} + \bar{R}_3 = -\kappa(L)\nabla u(A)|_L \cdot \bar{n}_{L K} + \bar{R}_4 \equiv f_2,$$

$$(2.21) \quad \kappa(L)\nabla u(A)|_L \cdot \bar{n}_{L L_A} + \bar{R}_5 = -\kappa(L_A)\nabla u(A)|_{L_A} \cdot \bar{n}_{L_A L} + \bar{R}_6 \equiv f_3,$$

$$(2.22) \quad \kappa(L_A)\nabla u(A)|_{L_A} \cdot \bar{n}_{L_A K_A} + \bar{R}_7 = -\kappa(K_A)\nabla u(A)|_{K_A} \cdot \bar{n}_{K_A L_A} + \bar{R}_8 \equiv f_4.$$

Here  $\bar{n}_{K_A K}$  is the unit normal vector to the common side of cells  $K_A$  and  $K$  with the direction from  $K_A$  to  $K$  (the others have similar definitions), and  $\bar{R}_i = O(h)$ , ( $i = 1, 2, \dots, 8$ ).

From (2.19) and (2.22), we have

$$\begin{cases} \bar{n}_{K_A K}^T \cdot \nabla u(A)|_{K_A} = \frac{f_1 - \bar{R}_1}{\kappa(K_A)}, \\ \bar{n}_{K_A L_A}^T \cdot \nabla u(A)|_{K_A} = -\frac{f_4 - \bar{R}_8}{\kappa(K_A)}. \end{cases}$$

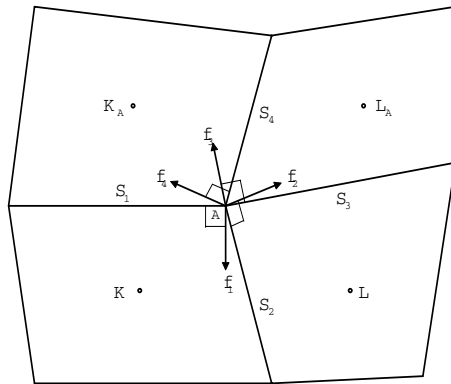


FIG. 2.3. The normal flux at vertex  $A$ .

This system of equations can be written as

$$X \nabla u(A)|_{K_A} = \begin{bmatrix} \frac{f_1 - \bar{R}_1}{\kappa(K_A)} \\ -\frac{f_4 - \bar{R}_8}{\kappa(K_A)} \end{bmatrix},$$

where

$$X = \begin{bmatrix} \vec{n}_{K_A K}^T \\ \vec{n}_{K_A L_A}^T \end{bmatrix}.$$

Introduce the matrix

$$R = \begin{bmatrix} 0 & 1 \\ -1 & 0 \end{bmatrix}.$$

Then, the determinant of  $X$  is  $T_{K_A} = \det X = \vec{n}_{K_A K}^T \cdot R \vec{n}_{K_A L_A}$ .  $T_{K_A}$  is equal to twice the area of the triangle spanned by the vectors  $\vec{n}_{K_A K}$  and  $\vec{n}_{K_A L_A}$  (the vectors  $\vec{n}_{K_A K}$  and  $\vec{n}_{K_A L_A}$  form a right-handed system). The inverse of matrix  $X$  is given by

$$X^{-1} = \frac{1}{T_{K_A}} [R \vec{n}_{K_A L_A}, -R \vec{n}_{K_A K}].$$

It follows that

$$(2.23) \quad \nabla u(A)|_{K_A} = \frac{1}{\kappa(K_A)T_{K_A}} R \vec{n}_{K_A L_A} (f_1 - \bar{R}_1) + \frac{1}{\kappa(K_A)T_{K_A}} R \vec{n}_{K_A K} (f_4 - \bar{R}_8).$$

In the same way, we have

$$(2.24) \quad \nabla u(A)|_K = \frac{1}{\kappa(K)T_K} R \vec{n}_{K K_A} (f_2 - \bar{R}_3) + \frac{1}{\kappa(K)T_K} R \vec{n}_{K L} (f_1 - \bar{R}_2),$$

$$(2.25) \quad \nabla u(A)|_L = \frac{1}{\kappa(L)T_L} R \vec{n}_{L K} (f_3 - \bar{R}_5) + \frac{1}{\kappa(L)T_L} R \vec{n}_{L L_A} (f_2 - \bar{R}_4),$$

$$(2.26) \quad \nabla u(A)|_{L_A} = \frac{1}{\kappa(L_A)T_{L_A}} R \vec{n}_{L_A L} (f_4 - \bar{R}_7) + \frac{1}{\kappa(L_A)T_{L_A}} R \vec{n}_{L_A K_A} (f_3 - \bar{R}_6),$$

where  $T_K = \vec{n}_{K L}^T \cdot R \vec{n}_{K K_A}$ ,  $T_L = \vec{n}_{L L_A}^T \cdot R \vec{n}_{L K}$ , and  $T_{L_A} = \vec{n}_{L_A K_A}^T \cdot R \vec{n}_{L_A L}$ .

Substitute (2.23) into (2.15) to obtain

$$(2.27) \quad u(K_A) = u(A) + \omega_{K_A,4} f_4 + \omega_{K_A,1} f_1 + \bar{R}'_{K_A},$$

where

$$\omega_{K_A,4} = \frac{1}{\kappa(K_A)T_{K_A}} |K_A - A| \cos \theta_2, \quad \omega_{K_A,1} = -\frac{1}{\kappa(K_A)T_{K_A}} |K_A - A| \cos \theta_1,$$

and  $\bar{R}'_{K_A} = O(h^2)$ . Here  $\theta_1$  and  $\theta_2$  are the angles between the segment  $K_A A$  and two cell sides (see Figure 2.4). Similarly, substitute (2.24), (2.25), and (2.26) into (2.16), (2.17), and (2.18), respectively, to obtain

$$(2.28) \quad u(K) = u(A) + \omega_{K,1} f_1 + \omega_{K,2} f_2 + \bar{R}'_K,$$

$$(2.29) \quad u(L) = u(A) + \omega_{L,2} f_2 + \omega_{L,3} f_3 + \bar{R}'_L,$$

$$(2.30) \quad u(L_A) = u(A) + \omega_{L_A,3} f_3 + \omega_{L_A,4} f_4 + \bar{R}'_{L_A},$$

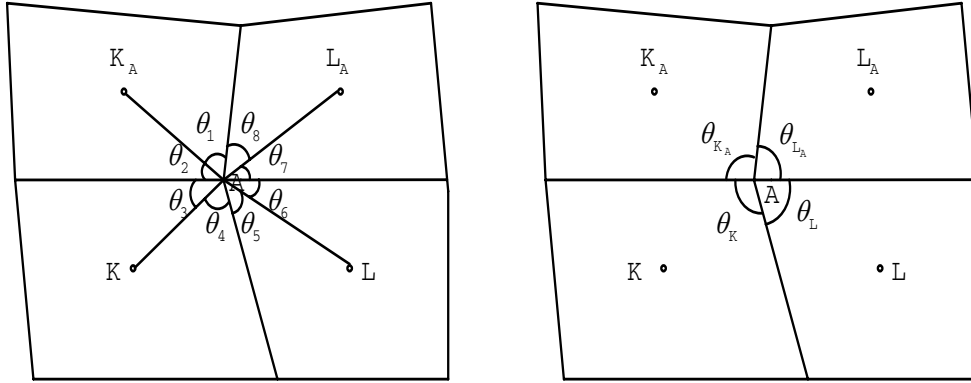


FIG. 2.4. The angles associated with vertex  $A$ .

where

$$\begin{aligned} \omega_{K,1} &= \frac{1}{\kappa(K)T_K} |K - A| \cos \theta_4, & \omega_{K,2} &= -\frac{1}{\kappa(K)T_K} |K - A| \cos \theta_3, \\ \omega_{L,2} &= \frac{1}{\kappa(L)T_L} |L - A| \cos \theta_6, & \omega_{L,3} &= -\frac{1}{\kappa(L)T_L} |L - A| \cos \theta_5, \\ \omega_{L_A,3} &= \frac{1}{\kappa(L_A)T_{L_A}} |L_A - A| \cos \theta_8, & \omega_{L_A,4} &= -\frac{1}{\kappa(L_A)T_{L_A}} |L_A - A| \cos \theta_7, \end{aligned}$$

and  $\bar{R}'_K, \bar{R}'_L$ , and  $\bar{R}'_{L_A}$  are all  $O(h^2)$ .

Multiply (2.27)–(2.30) by  $\omega_{A_i}$  ( $i = 1, 2, 3, 4$ ), respectively, and add the resulting equations to obtain

$$\begin{aligned} & \omega_{A_1} u(K_A) + \omega_{A_2} u(K) + \omega_{A_3} u(L) + \omega_{A_4} u(L_A) \\ &= \sum_{i=1}^4 \omega_{A_i} u(A) + (\omega_{A_1} \omega_{K_A,1} + \omega_{A_2} \omega_{K,1}) f_1 + (\omega_{A_2} \omega_{K,2} + \omega_{A_3} \omega_{L,2}) f_2 \\ (2.31) \quad & + (\omega_{A_3} \omega_{L,3} + \omega_{A_4} \omega_{L_A,3}) f_3 + (\omega_{A_4} \omega_{L_A,4} + \omega_{A_1} \omega_{K_A,4}) f_4 + \bar{R}_A, \end{aligned}$$

where  $\bar{R}_A = O(h^2)$ .

In order to obtain second-order approximation, the coefficients of  $f_1, f_2, f_3$ , and  $f_4$  should be zero, and the coefficient of  $u(A)$  should be 1, which leads to five equations about  $\omega_{A_i}$ . However, there are only four unknowns  $\omega_{A_i}$  ( $i = 1, \dots, 4$ ).

Note that the five equations are not independent. We will find their relations by the continuity of the tangential gradients on the cell side. Specifically, the tangential gradient on the edge  $S_1$ , which is the common edge of the cells  $K$  and  $K_A$ , is continuous; that is,

$$(2.32) \quad \nabla u(A)|_{K_A} \cdot (-R\vec{n}_{K_A K}) = \nabla u(A)|_K \cdot (R\vec{n}_{K K_A}).$$

Substitute (2.23) and (2.24) into the above equation to obtain

$$(2.33) \quad a_1 f_1 + a_2 f_4 = a_3 f_2 + a_4 f_1 + (a_1 \bar{R}_1 + a_2 \bar{R}_8 - a_3 \bar{R}_3 - a_4 \bar{R}_2),$$

where  $a_1 = \frac{\cos \theta_{K_A}}{\kappa(K_A)T_{K_A}}$ ,  $a_2 = -\frac{1}{\kappa(K_A)T_{K_A}}$ ,  $a_3 = \frac{1}{\kappa(K)T_K}$ , and  $a_4 = -\frac{\cos \theta_K}{\kappa(K)T_K}$ . Here  $\theta_{K_A}$  and  $\theta_K$  are shown in Figure 2.4.

Similarly, note that the tangential gradients on the edge  $S_i$  ( $i = 2, 3, 4$ ) are continuous, respectively; that is,

$$\begin{aligned} \nabla u(A)|_K \cdot (-R\vec{n}_{KL}) &= \nabla u(A)|_L \cdot (R\vec{n}_{LK}), \\ \nabla u(A)|_L \cdot (-R\vec{n}_{LLA}) &= \nabla u(A)|_{L_A} \cdot (R\vec{n}_{L_A L}), \\ \nabla u(A)|_{L_A} \cdot (-R\vec{n}_{L_A K_A}) &= \nabla u(A)|_{K_A} \cdot (R\vec{n}_{K_A L_A}). \end{aligned}$$

It follows that

$$(2.34) \quad b_1 f_2 + b_2 f_1 = b_3 f_3 + b_4 f_2 + (b_1 \bar{R}_3 + b_2 \bar{R}_2 - b_3 \bar{R}_5 - b_4 \bar{R}_4),$$

$$(2.35) \quad c_1 f_3 + c_2 f_2 = c_3 f_4 + c_4 f_3 + (c_1 \bar{R}_5 + c_2 \bar{R}_4 - c_3 \bar{R}_7 - c_4 \bar{R}_6),$$

$$(2.36) \quad d_1 f_4 + d_2 f_3 = d_3 f_1 + d_4 f_4 + (d_1 \bar{R}_7 + d_2 \bar{R}_6 - d_3 \bar{R}_1 - d_4 \bar{R}_8).$$

Here

$$\begin{aligned} b_1 &= \frac{\cos \theta_K}{\kappa(K)T_K}, & b_2 &= -\frac{1}{\kappa(K)T_K}, & b_3 &= \frac{1}{\kappa(L)T_L}, & b_4 &= -\frac{\cos \theta_L}{\kappa(L)T_L}, \\ c_1 &= \frac{\cos \theta_L}{\kappa(L)T_L}, & c_2 &= -\frac{1}{\kappa(L)T_L}, & c_3 &= \frac{1}{\kappa(L_A)T_{L_A}}, & c_4 &= -\frac{\cos \theta_{L_A}}{\kappa(L_A)T_{L_A}}, \\ d_1 &= \frac{\cos \theta_{L_A}}{\kappa(L_A)T_{L_A}}, & d_2 &= -\frac{1}{\kappa(L_A)T_{L_A}}, & d_3 &= \frac{1}{\kappa(K_A)T_{K_A}}, & d_4 &= -\frac{\cos \theta_{K_A}}{\kappa(K_A)T_{K_A}}. \end{aligned}$$

From (2.33)–(2.36), we can find the relation between  $f_{i_0}$  and  $f_i$  ( $i \neq i_0$ ). Specifically, we can obtain the relation between  $f_2$  and  $f_1, f_4$  from (2.33),

$$(2.37) \quad f_2 = t_1 f_1 + t_2 f_4 + R_{s_1},$$

where  $t_1 = \frac{a_1 - a_4}{a_3}$ ,  $t_2 = \frac{a_2}{a_3}$ , and  $R_{s_1} = O(h)$ . Substitute the relation (2.37) into (2.31) to obtain

$$\begin{aligned} \omega_{A_1} u(K_A) + \omega_{A_2} u(K) + \omega_{A_3} u(L) + \omega_{A_4} u(L_A) &= \sum_{i=1}^4 \omega_{A_i} u(A) \\ &+ (\omega_{A_1} \omega_{K_A,1} + \omega_{A_2} (\omega_{K,1} + \omega_{K,2} t_1) + \omega_{A_3} \omega_{L,2} t_1) f_1 + (\omega_{A_3} \omega_{L,3} + \omega_{A_4} \omega_{L_A,3}) f_3 \\ (2.38) \quad &+ (\omega_{A_4} \omega_{L_A,4} + \omega_{A_1} \omega_{K_A,4} + \omega_{A_2} \omega_{K,2} t_2 + \omega_{A_3} \omega_{L,2} t_2) f_4 + \bar{R}'_A, \end{aligned}$$

where  $\bar{R}'_A = O(h^2)$ .

Letting the coefficients of  $f_1, f_3$ , and  $f_4$  be zero, we obtain four equations about four unknowns  $\omega_{A_i}$  ( $i = 1, \dots, 4$ ). It follows that

$$u(A) = \omega_{A_1} u(K_A) + \omega_{A_2} u(K) + \omega_{A_3} u(L) + \omega_{A_4} u(L_A) + R'_A,$$

where  $R'_A = -\bar{R}'_A = O(h^2)$ .

Similarly, we can obtain the relation between  $f_{i_0}$  and  $f_i$  ( $i \neq i_0$ ) from (2.34) or (2.35) or (2.36). Substitute this relation into (2.31) and let the coefficients of  $f_i$  be zero; then we can obtain the expression of  $u(A)$ .

It is obvious that we obtain four different expressions of  $u(A)$  with four groups of combination coefficients  $(\omega_{A_1}^{(j)}, \omega_{A_2}^{(j)}, \omega_{A_3}^{(j)}, \omega_{A_4}^{(j)})$  ( $1 \leq j \leq 4$ ). In order to make the expression of  $u(A)$  unique, we simply take  $\omega = \omega^{(j_0)}$  such that

$$(2.39) \quad \sum_{i=1}^4 |\omega_{A_i}^{(j_0)}| = \min_{1 \leq j \leq 4} \sum_{i=1}^4 |\omega_{A_i}^{(j)}|.$$

Hence, we get the unique expression of  $u(A)$  as follows:

$$(2.40) \quad u(A) = \omega_{A_1} u(K_{A_1}) + \omega_{A_2} u(K) + \omega_{A_3} u(L) + \omega_{A_4} u(L_A) + R_A,$$

where  $R_A = O(h^2)$ .

**2.4. The nine point scheme.** Substituting the expression of vertex unknowns into (2.10), we have

$$\begin{aligned} \mathcal{F}_{K,\sigma} = & -\tau_\sigma \{u(L) - u(K) - D_\sigma [\omega_{A_1} u(K_{A_1}) + \omega_{A_2} u(K) + \omega_{A_3} u(L) + \omega_{A_4} u(L_A)] \\ & - (\omega_{B_1} u(K) + \omega_{B_2} u(K_B) + \omega_{B_3} u(L_B) + \omega_{B_4} u(L))\} + W_{K,\sigma}, \end{aligned}$$

where  $W_{K,\sigma} = O(h^2)$ . Denote

$$\begin{aligned} \bar{F}_{K,\sigma} = & -\tau_\sigma \{u(L) - u(K) - D_\sigma [\omega_{A_1} u(K_{A_1}) + \omega_{A_2} u(K) + \omega_{A_3} u(L) + \omega_{A_4} u(L_A)] \\ & - (\omega_{B_1} u(K) + \omega_{B_2} u(K_B) + \omega_{B_3} u(L_B) + \omega_{B_4} u(L))\}. \end{aligned}$$

Therefore,  $\mathcal{F}_{K,\sigma}^{n+1} = \bar{F}_{K,\sigma}^{n+1} + W_{K,\sigma}$ .

Let

$$(2.41) \quad \begin{aligned} F_{K,\sigma} = & -\tau_\sigma \{u_L - u_K - D_\sigma [\omega_{A_1} u_{K_{A_1}} + \omega_{A_2} u_K + \omega_{A_3} u_L + \omega_{A_4} u_{L_A}] \\ & - (\omega_{B_1} u_K + \omega_{B_2} u_{K_B} + \omega_{B_3} u_{L_B} + \omega_{B_4} u_L)\}; \end{aligned}$$

then the finite volume scheme of the problem (2.1)–(2.2) is given as follows:

$$(2.42) \quad \sum_{\sigma \in \mathcal{E}_K} F_{K,\sigma} = f_K m(K), \quad K \in \Omega,$$

$$(2.43) \quad u_K = 0, \quad K \in \partial\Omega,$$

where  $f_K = f(K)$ , and  $K \in \partial\Omega$  means that  $K$  is a boundary edge and also the midpoint of the boundary edge.

It is obvious that the scheme at cell  $K$  is coupled with the eight cells around it; hence there are nine cells in our stencil (see Figure 2.5), so we call the scheme a nine point scheme. Our scheme reduces to the standard five point scheme on rectangular grids (see Figure 2.6). The scheme often leads to a system with a nonsymmetric matrix for general quadrilateral meshes. It is straightforward to extend our scheme on distorted quadrilateral meshes to arbitrary polygonal meshes.

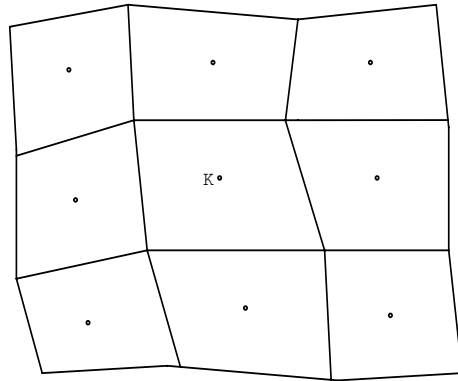


FIG. 2.5. *Nine point stencil.*

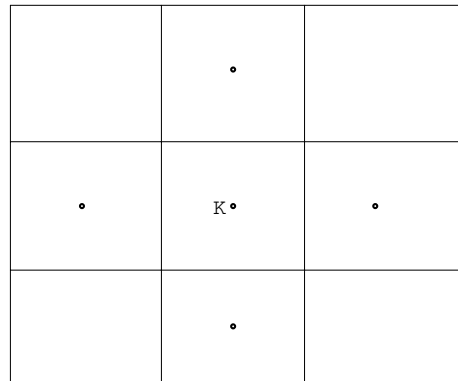


FIG. 2.6. *Five point stencil.*

**3. Stability and convergence of scheme.** In order to obtain the theorems of stability and convergence, we introduce the following assumption (H3):

$$\begin{aligned} \tau_\sigma D_\sigma^2 \omega_{A_1}^2 &\leq \frac{1 - \varepsilon_0 - \varepsilon}{16} \tau_{K_A|K}, & \tau_\sigma D_\sigma^2 \omega_{A_4}^2 &\leq \frac{1 - \varepsilon_0 - \varepsilon}{16} \tau_{L_A|L}, \\ \tau_\sigma D_\sigma^2 \omega_{B_2}^2 &\leq \frac{1 - \varepsilon_0 - \varepsilon}{16} \tau_{K|K_B}, & \tau_\sigma D_\sigma^2 \omega_{B_3}^2 &\leq \frac{1 - \varepsilon_0 - \varepsilon}{16} \tau_{L|L_B}, \\ D_\sigma(\omega_{A_3} + \omega_{A_4} - \omega_{B_3} - \omega_{B_4}) &\leq \frac{\varepsilon_0}{2}, \end{aligned}$$

where  $\varepsilon_0 \in (0, 1)$  is a given constant, and  $\varepsilon > 0$  is a small constant satisfying  $\varepsilon_0 + \varepsilon < 1$ .

The above assumption (H3) implies a geometric constraint on cell deformation. For an orthogonal mesh,  $D_\sigma = 0$ . The inequality  $\tau_\sigma D_\sigma^2 \omega_{A_1}^2 \leq \frac{1 - \varepsilon_0 - \varepsilon}{16} \tau_{K_A|K}$  can be rewritten as  $\frac{\tau_\sigma}{\tau_{K_A|K}} D_\sigma^2 \omega_{A_1}^2 \leq \frac{1 - \varepsilon_0 - \varepsilon}{16}$ . When  $\kappa = 1$ , we have  $\tau_\sigma = \frac{|A-B|}{|K-L| \cos \theta}$ ,  $D_\sigma = \frac{|L-K| \sin \theta}{|A-B|}$ . It is obvious that the assumption is a constraint on some geometric parameters, which include the angle between the cell side and the segment connecting neighboring cell centers, and the ratio between the length of the cell side and the length of the segment connecting neighboring cell centers.

**3.1. Stability.** Now we prove that our scheme is stable.

**THEOREM 3.1.** *Assume that (H1), (H2), and (H3) are satisfied. Then there exists a constant C, independent of h, such that*

$$\sum_{\sigma \in \mathcal{E}} \tau_{\sigma} (u_L - u_K)^2 \leq C \sum_{K \in \mathcal{J}} |f_K|^2 m(K).$$

*Proof.* Multiplying (2.42) by  $u_K$  and summing up the resulting products for  $K \in \mathcal{J}$ , we get

$$(3.1) \quad \sum_{K \in \mathcal{J}} \sum_{\sigma \in \mathcal{E}_K} F_{K,\sigma} u_K = \sum_{K \in \mathcal{J}} f_K u_K m(K).$$

Notice that

$$\begin{aligned} \sum_{K \in \mathcal{J}} \sum_{\sigma \in \mathcal{E}_K} F_{K,\sigma} u_K &= - \sum_{K \in \mathcal{J}} \sum_{\sigma \in \mathcal{E}_K} \tau_{\sigma} (u_L - u_K - D_{\sigma}(\omega_{A_1} u_{K_A} + \omega_{A_2} u_K + \omega_{A_3} u_L \\ &\quad + \omega_{A_4} u_{L_A} - (\omega_{B_1} u_K + \omega_{B_2} u_{K_B} + \omega_{B_3} u_{L_B} + \omega_{B_4} u_L))) u_K \\ &= \sum_{\sigma \in \mathcal{E}} \tau_{\sigma} (u_L - u_K)^2 + \sum_{\sigma \in \mathcal{E}_{int}} \tau_{\sigma} D_{\sigma}(\omega_{A_1} u_{K_A} + \omega_{A_2} u_K + \omega_{A_3} u_L \\ &\quad + \omega_{A_4} u_{L_A} - (\omega_{B_1} u_K + \omega_{B_2} u_{K_B} + \omega_{B_3} u_{L_B} + \omega_{B_4} u_L))(u_K - u_L) \\ &= \sum_{\sigma \in \mathcal{E}} \tau_{\sigma} (u_L - u_K)^2 + \sum_{\sigma \in \mathcal{E}_{int}} \tau_{\sigma} D_{\sigma}(\omega_{A_1} (u_{K_A} - u_K) \\ &\quad + \omega_{A_4} (u_{L_A} - u_L) \\ &\quad + \omega_{B_2} (u_K - u_{K_B}) + \omega_{B_3} (u_L - u_{L_B}) + (\omega_{A_2} + \omega_{A_1} - \omega_{B_1} - \omega_{B_2}) \\ &\quad \cdot u_K + (\omega_{A_3} + \omega_{A_4} - \omega_{B_3} - \omega_{B_4}) u_L)(u_K - u_L) \\ &= \sum_{\sigma \in \mathcal{E}} \tau_{\sigma} (u_L - u_K)^2 + \sum_{\sigma \in \mathcal{E}_{int}} \tau_{\sigma} D_{\sigma}(\omega_{A_1} (u_{K_A} - u_K) \\ &\quad + \omega_{A_4} (u_{L_A} - u_L) + \omega_{B_2} (u_K - u_{K_B}) \\ &\quad + \omega_{B_3} (u_L - u_{L_B}))(u_K - u_L) \\ (3.2) \quad &- \sum_{\sigma \in \mathcal{E}_{int}} \tau_{\sigma} D_{\sigma}(\omega_{A_3} + \omega_{A_4} - \omega_{B_3} - \omega_{B_4})(u_K - u_L)^2. \end{aligned}$$

Substitute (3.2) into (3.1) to obtain

$$\begin{aligned} \sum_{\sigma \in \mathcal{E}} \tau_{\sigma} (u_L - u_K)^2 - \sum_{\sigma \in \mathcal{E}_{int}} \tau_{\sigma} D_{\sigma}(\omega_{A_3} + \omega_{A_4} - \omega_{B_3} - \omega_{B_4})(u_K - u_L)^2 \\ + \sum_{\sigma \in \mathcal{E}_{int}} \tau_{\sigma} D_{\sigma}(\omega_{A_1} (u_{K_A} - u_K) + \omega_{A_4} (u_{L_A} - u_L) + \omega_{B_2} (u_K - u_{K_B}) \\ (3.3) \quad + \omega_{B_3} (u_L - u_{L_B}))(u_K - u_L) = \sum_{K \in \mathcal{J}} f_K u_K m(K). \end{aligned}$$

By the Cauchy inequality,

$$\begin{aligned} & \sum_{\sigma \in \mathcal{E}} \tau_\sigma (u_L - u_K)^2 - \sum_{\sigma \in \mathcal{E}_{int}} \tau_\sigma D_\sigma (\omega_{A_3} + \omega_{A_4} - \omega_{B_3} - \omega_{B_4}) (u_K - u_L)^2 \\ & \leq \sum_{\sigma \in \mathcal{E}_{int}} \frac{1}{2} \tau_\sigma (u_L - u_K)^2 + 2 \sum_{\sigma \in \mathcal{E}_{int}} \tau_\sigma D_\sigma^2 (\omega_{A_1}^2 (u_{K_A} - u_K)^2 + \omega_{A_4}^2 (u_{L_A} - u_L)^2 \\ & \qquad \qquad \qquad + \omega_{B_2}^2 (u_K - u_{K_B})^2 + \omega_{B_3}^2 (u_L - u_{L_B})^2) \\ & \quad + \frac{C}{\varepsilon} \sum_{K \in \mathcal{J}} |f_K|^2 m(K) + \frac{\varepsilon}{4C} \sum_{K \in \mathcal{J}} |u_K|^2 m(K). \end{aligned}$$

Apply the assumption (H3) and the Sobolev inequality to obtain

$$\sum_{\sigma \in \mathcal{E}} \frac{\varepsilon}{4} \tau_\sigma (u_L - u_K)^2 \leq \frac{C}{\varepsilon} \sum_{K \in \mathcal{J}} |f_K|^2 m(K),$$

and hence,

$$\sum_{\sigma \in \mathcal{E}} \tau_\sigma (u_L - u_K)^2 \leq C \sum_{K \in \mathcal{J}} |f_K|^2 m(K).$$

Thus the scheme (2.42)–(2.43) is stable.  $\square$

**3.2. Convergence.** Equation (2.3) is equivalent to the following equation:

$$(3.4) \quad \sum_{\sigma \in \mathcal{E}_K} \mathcal{F}_{K,\sigma} = f_K m(K) + S_K m(K),$$

where  $f_K = f(K)$ ,  $S_K = \int_K (f(x) - f_K) dx / m(K)$ . Obviously,  $|S_K| \leq Ch$  by assumption (H1).

Let  $e_K = u(K) - u_K$ , and subtract (2.42) from (3.4) to obtain

$$(3.5) \quad \sum_{\sigma \in \mathcal{E}_K} G_{K,\sigma} = S_K m(K) - \sum_{\sigma \in \mathcal{E}_K} W_{K,\sigma},$$

where  $G_{K,\sigma} = \bar{F}_{K,\sigma} - F_{K,\sigma}$ .

Now we present an error estimate for the scheme (2.42)–(2.43).

**THEOREM 3.2.** *Assume that (H1), (H2), and (H3) are satisfied. Then there exists a constant  $C$ , independent of  $h$ , such that*

$$\left( \sum_{\sigma \in \mathcal{E}} \tau_\sigma (e_L - e_K)^2 \right)^{1/2} \leq Ch.$$

*Proof.* Multiplying (3.5) by  $e_K$ , and summing up the resulting products for  $K \in \mathcal{J}$ , we get

$$(3.6) \quad \sum_{K \in \mathcal{J}} \sum_{\sigma \in \mathcal{E}_K} G_{K,\sigma} e_K = \sum_{K \in \mathcal{J}} S_K e_K m(K) - \sum_{K \in \mathcal{J}} \sum_{\sigma \in \mathcal{E}_K} W_{K,\sigma} e_K.$$

Notice that

$$\begin{aligned}
 \sum_{K \in \mathcal{J}} \sum_{\sigma \in \mathcal{E}_K} G_{K,\sigma} e_K &= - \sum_{\sigma \in \mathcal{E}_{int}} \tau_\sigma D_\sigma (\omega_{A_3} + \omega_{A_4} - \omega_{B_3} - \omega_{B_4}) (e_K - e_L)^2 \\
 &\quad + \sum_{\sigma \in \mathcal{E}} \tau_\sigma (e_L - e_K)^2 + \sum_{\sigma \in \mathcal{E}_{int}} \tau_\sigma D_\sigma (\omega_{A_1} (e_{K_A} - e_K) \\
 (3.7) \quad &\quad + \omega_{A_4} (e_{L_A} - e_L) + \omega_{B_2} (e_K - e_{K_B}) + \omega_{B_3} (e_L - e_{L_B})) (e_K - e_L).
 \end{aligned}$$

Denote  $W_\sigma = W_{K,\sigma}$ , notice that  $W_{L,\sigma} = -W_{K,\sigma}$ , and substitute (3.7) into (3.6) to obtain

$$\begin{aligned}
 &\sum_{\sigma \in \mathcal{E}} \tau_\sigma (e_L - e_K)^2 - \sum_{\sigma \in \mathcal{E}_{int}} \tau_\sigma D_\sigma (\omega_{A_3} + \omega_{A_4} - \omega_{B_3} - \omega_{B_4}) (e_K - e_L)^2 \\
 &\quad + \sum_{\sigma \in \mathcal{E}_{int}} \tau_\sigma D_\sigma (\omega_{A_1} (e_{K_A} - e_{K_A}) + \omega_{A_4} (e_{L_A} - e_L) + \omega_{B_2} (e_K - e_{K_B}) \\
 &\quad \quad \quad + \omega_{B_3} (e_L - e_{L_B})) (e_K - e_L) \\
 &= \sum_{K \in \mathcal{J}} S_K e_K m(K) - \sum_{\sigma \in \mathcal{E}} W_\sigma (e_K - e_L).
 \end{aligned}$$

By the Cauchy inequality, we have

$$\begin{aligned}
 &\sum_{\sigma \in \mathcal{E}} \tau_\sigma (e_L - e_K)^2 - \sum_{\sigma \in \mathcal{E}_{int}} \tau_\sigma D_\sigma (\omega_{A_3} + \omega_{A_4} - \omega_{B_3} - \omega_{B_4}) (e_K - e_L)^2 \\
 &\leq \sum_{\sigma \in \mathcal{E}_{int}} \frac{1}{2} \tau_\sigma (e_L - e_K)^2 + 2 \sum_{\sigma \in \mathcal{E}_{int}} \tau_\sigma D_\sigma^2 [\omega_{A_1}^2 (e_{K_A} - e_K)^2 + \omega_{A_4}^2 (e_{L_A} - e_L)^2 \\
 &\quad + \omega_{B_2}^2 (e_K - e_{K_B})^2 + \omega_{B_3}^2 (e_L - e_{L_B})^2] + \sum_{\sigma \in \mathcal{E}} \frac{\varepsilon}{8} \tau_\sigma (e_K - e_L)^2 \\
 &\quad + \sum_{\sigma \in \mathcal{E}} \frac{2}{\varepsilon \tau_\sigma} |W_\sigma|^2 + \frac{\varepsilon}{8C_1} \sum_{K \in \mathcal{J}} |e_K|^2 m(K) + Ch^2.
 \end{aligned}$$

Applying the assumption (H3) and the Sobolev inequality, we obtain

$$\sum_{\sigma \in \mathcal{E}} \tau_\sigma (u_L - u_K)^2 \leq Ch^2. \quad \square$$

**4. Extension to general model diffusion equation.** Consider now the general model diffusion problem

$$(4.1) \quad -\nabla \cdot (\kappa(x) \nabla u) = f(x) \quad \text{in } \Omega,$$

$$(4.2) \quad u(x) = 0 \quad \text{on } \partial\Omega,$$

where  $\kappa(x)$  is a positive definite  $2 \times 2$  matrix.

Making the same operations as those at the beginning of subsection 2.2, and noticing that

$$(\kappa \nabla u) \cdot \nu = \nabla u \cdot (\kappa^t \nu),$$

we obtain

$$(4.3) \quad \sum_{\sigma \in \mathcal{E}_K} \mathcal{F}_{K,\sigma} = \int_K f(x) dx,$$

where

$$(4.4) \quad \mathcal{F}_{K,\sigma} = - \int_{\sigma} \nabla u(x) \cdot \kappa(x)^t \vec{n}_{K,\sigma} dl.$$

Since vectors  $\vec{\tau}_{BA}$  and  $\vec{\tau}_{KI}$  cannot be collinear, there exist  $\alpha(x)$  and  $\beta(x)$  depending on  $\kappa$  such that

$$(4.5) \quad \kappa(x)^t \vec{n}_{K,\sigma} = -\alpha(x) \vec{\tau}_{BA} + \beta(x) \vec{\tau}_{KI},$$

where

$$\alpha(x) = \frac{1}{\cos \theta_{K,\sigma}} \vec{\nu}_{KI} \cdot (\kappa(x)^t \vec{n}_{K,\sigma}), \quad \beta(x) = \frac{1}{\cos \theta_{K,\sigma}} \vec{n}_{K,\sigma} \cdot (\kappa(x)^t \vec{n}_{K,\sigma}).$$

Using a similar derivation as in section 2, we have

$$\mathcal{F}_{K,\sigma} = -\tau_{\sigma} \{u(L) - u(K) - D_{\sigma} [u(A) - u(B)]\} + R_{K,\sigma},$$

$$\mathcal{F}_{L,\sigma} = -\tau_{\sigma} \{u(K) - u(L) - D_{\sigma} [u(B) - u(A)]\} + R_{L,\sigma},$$

where  $\tau_{\sigma} = \frac{|A-B|}{\frac{|I-K|}{\beta(K)} + \frac{|I-L|}{\beta(L)}}$ ,  $D_{\sigma} = \frac{|I-K|\alpha(K)}{|A-B|\beta(K)} + \frac{|I-L|\alpha(L)}{|A-B|\beta(L)}$ , and  $R_{K,\sigma} = -R_{L,\sigma} = O(h^2)$ .

Let

$$F_{K,\sigma} = -\tau_{\sigma} \{u_L - u_K - D_{\sigma} [\omega_{A_1} u_{K_A} + \omega_{A_2} u_K + \omega_{A_3} u_L + \omega_{A_4} u_{L_A} - (\omega_{B_1} u_K + \omega_{B_2} u_{K_B} + \omega_{B_3} u_{L_B} + \omega_{B_4} u_L)]\},$$

where  $\omega_{A_i}$  and  $\omega_{B_i}$  satisfy relations similar to those in section 2. Then we obtain the finite volume scheme of problem (4.1)–(4.2). It is obvious that we have theorems similar to those in section 3.

**5. Numerical experiments.** Let us now present some numerical results to illustrate the behavior of the proposed finite volume scheme.

The symmetric linear systems are solved by the conjugate gradient (CG) method, and the nonsymmetric linear systems are solved by the biconjugate gradient stabilized algorithm (BICGSTAB) (see [14]).

Let  $\Omega$  be the unit square, and let  $\partial\Omega_S, \partial\Omega_E, \partial\Omega_N, \partial\Omega_W$  be the boundaries of  $\Omega$ . The first distorted mesh is a random mesh (see [8]). The random mesh over the physical domain  $\Omega = [0, 1] \times [0, 1]$  is defined by  $x_{ij} = \frac{i}{J} + \frac{\sigma}{J}(R_x - 0.5)$ ,  $y_{ij} = \frac{j}{J} + \frac{\sigma}{J}(R_y - 0.5)$ , where  $\sigma \in [0, 1]$  is a parameter and  $R_x$  and  $R_y$  are two normalized random variables. The second distorted mesh is a Z-mesh as described in [9]. Figure 5.1 displays a random mesh generated with  $\sigma = 0.7$  and a Z-mesh.

**5.1. Linear elliptic equation.** In order to test the scheme given in section 2 and compare it with some known methods, we consider the following linear elliptic equation whose analytic solution is  $u = 2 + \cos(\pi x) + \sin(\pi y)$ :

$$\begin{aligned} -\nabla \cdot (\nabla u) &= \pi^2(\cos(\pi x) + \sin(\pi y)) && \text{in } \Omega, \\ u &= 2 + \cos(\pi x) && \text{on } \partial\Omega_S \cup \partial\Omega_N, \\ \nabla u \cdot \nu &= 0 && \text{on } \partial\Omega_E \cup \partial\Omega_W. \end{aligned}$$

Table 5.1 gives the error between the exact solution and the numerical solution on the above mentioned random meshes, where NPCT (nine point scheme with cell-centered unknowns and Taylor expansion) is our new method, NPC is the method of [10] in which all of the combination coefficients are  $\frac{1}{4}$ , NPCV is the method of constructing the scheme on both cell centers and vertices (see [7, 19]), and MPFA is the method of multipoint flux approximations in [1]. NPCT, NPC, and MPFA lead to linear systems with a nonsymmetric matrix, and we use BICGSTAB to solve them. NPCV leads to a linear system with a symmetric matrix, and we use CG to solve it. From Table 5.1, one can see clearly that MPFA produces the best results for this case and exhibits nearly second-order convergence. NPCT produces the next best results for this case and also exhibits nearly second-order convergence. NPCV also has nearly second-order convergence, while NPC is the worst, failing to converge as the number of cells is increased. Compared with NPCV, our method not only provides more accurate results, but also is less expensive. This is because our method has less than half the unknowns of NPCV; i.e., our method has only the cell-centered unknowns, and NPCV has both cell-centered unknowns and vertex unknowns.

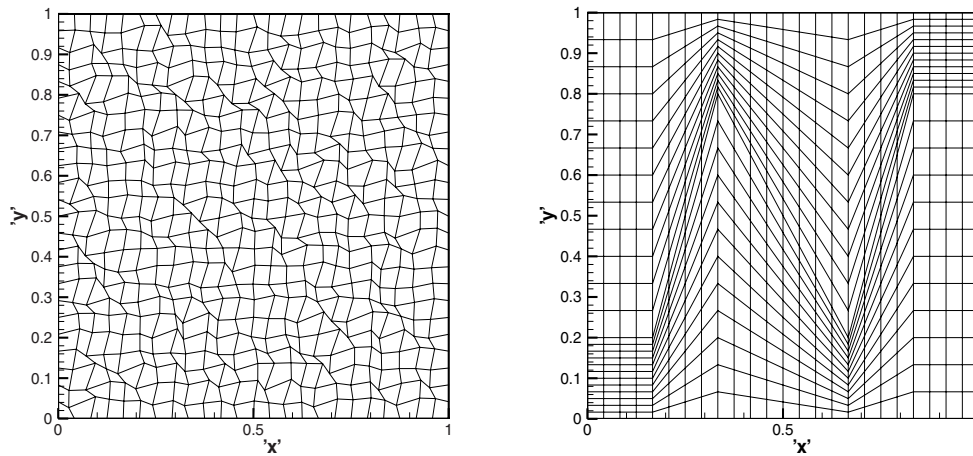
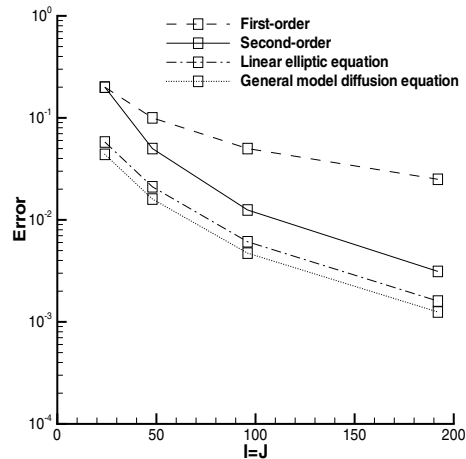


FIG. 5.1. Distorted quadrilateral mesh ( $24 \times 24$ ; left: random mesh, right: Z-mesh).

TABLE 5.1  
Results for the linear elliptic equation on a random mesh.

	$I \times J$	$12 \times 12$	$24 \times 24$	$48 \times 48$	$96 \times 96$	$192 \times 192$
NPCT	Maximum error	1.59e-2	4.01e-3	1.07e-3	3.05e-4	8.74e-5
	time(s)	–	–	0.25	2.43	28.85
MPFA	Maximum error	1.49E-2	3.58E-3	1.05E-3	2.72E-4	6.99E-5
	time(s)	–	–	0.28	2.02	24.55
NPCV	Maximum error	1.67e-2	4.28e-3	1.25e-3	3.30e-4	9.31e-5
	time(s)	–	–	0.40	3.63	57.94
NPC	Maximum error	0.23	0.15	0.14	0.14	0.14
	time(s)	–	–	0.22	2.62	37.08

Figure 5.2 displays the error between the exact solution and the numerical solution for the above-mentioned Z-mesh. The dashed line refers to first-order convergence, the solid line refers to second-order convergence, and the dash-dotted line gives the error of our method for the linear elliptic equation. One can see clearly that our

FIG. 5.2. The results on  $Z$ -mesh.

method exhibits nearly second-order convergence in this case.

Although we proved our scheme to be first-order accurate in theory, numerical experiments show that it appears to be second-order accurate for the tested problems.

**5.2. The general model diffusion problem.** In this subsection, we consider the general model diffusion problem

$$\begin{aligned} -\nabla \cdot (\kappa(x)\nabla u) &= f(x) && \text{in } \Omega, \\ u &= \sin(\pi x) \sin(\pi y) && \text{on } \partial\Omega, \end{aligned}$$

where  $\kappa(x)$  is a symmetric positive definite matrix,  $\kappa(x) = RDR^T$ , and

$$R = \begin{pmatrix} \cos \theta & -\sin \theta \\ \sin \theta & \cos \theta \end{pmatrix}, \quad D = \begin{pmatrix} d_1 & 0 \\ 0 & d_2 \end{pmatrix},$$

$\theta = \frac{5\pi}{12}$ ,  $d_1 = 1 + 2x^2 + y^2$ ,  $d_2 = 1 + x^2 + 2y^2$ . The solution is chosen to be  $u(x, y) = \sin(\pi x) \sin(\pi y)$ .

TABLE 5.2  
Results for the general model diffusion problem.

	$I \times J$	$12 \times 12$	$24 \times 24$	$48 \times 48$	$96 \times 96$	$192 \times 192$
NPCT	Maximum error	9.65e-3	2.55e-3	8.21e-4	2.12e-4	5.46e-5
	time(s)	—	—	0.25	2.15	45.58
MPFA	Maximum error	1.50E-2	3.27E-3	9.53E-4	2.52E-4	6.97E-5
	time(s)	—	—	0.28	2.17	36.32
NPCV	Maximum error	1.30e-2	3.24e-3	9.32e-4	2.48e-4	7.36e-5
	time(s)	—	—	0.27	2.57	37.08
NPC	Maximum error	8.45e-2	9.42e-2	7.71e-2	8.39e-2	8.09e-2
	time(s)	—	—	0.23	2.12	40.77

Table 5.2 gives the error between the exact solution and the numerical solution. From this table, one can see that NPCT produces the best results for this case and

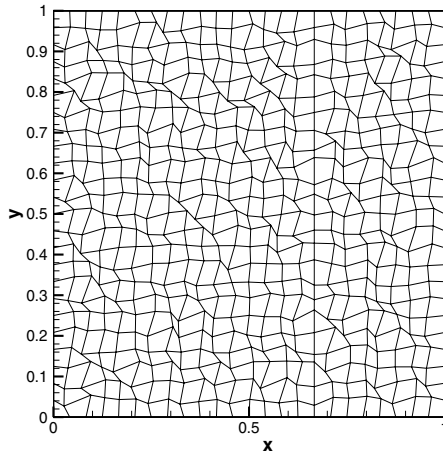


FIG. 5.3. Random mesh with a discontinuity in  $x = 2/3$  ( $24 \times 24$ ).

TABLE 5.3  
Results for the linear elliptic equation with discontinue coefficients.

	$I \times J$	$12 \times 12$	$24 \times 24$	$48 \times 48$	$96 \times 96$	$192 \times 192$
NPCT	Maximum error	8.56e-2	2.97e-2	1.04e-3	2.81e-3	8.01e-4
	time(s)	–	–	0.30	2.32	37.53
MPFA	Maximum error	9.10E-2	3.07E-2	1.03E-2	2.79E-3	8.22E-4
	time(s)	–	–	0.30	2.42	34.20
NPCV	Maximum error	1.81E-1	3.53E-2	1.12E-2	3.13E-3	8.63E-4
	time(s)	–	–	0.32	2.48	34.00

exhibits nearly second-order convergence. NPCV and MPFA produce the next best results for this case and also exhibit nearly second-order convergence, while NPC is the worst, failing to converge as the number of cells is increased. In Figure 5.2, the dotted line gives the error of our scheme for the general model diffusion equation on a Z-mesh. One can see clearly that our scheme exhibits nearly second-order convergence for this case.

**5.3. Linear elliptic equation with discontinuous coefficients.** Consider the following linear elliptic equation with discontinuous coefficients:

$$\begin{aligned}
 -\nabla \cdot (\kappa(x, y)\nabla u) &= f(x, y) && \text{in } \Omega, \\
 u(x, y) &= 0 && \text{on } \partial\Omega,
 \end{aligned}$$

where

$$\kappa(x, y) = \begin{cases} 4, & (x, y) \in (0, \frac{2}{3}] \times (0, 1), \\ 1, & (x, y) \in (\frac{2}{3}, 1) \times (0, 1), \end{cases}$$

and

$$f(x, y) = \begin{cases} 20\pi^2 \sin \pi x \sin 2\pi y, & (x, y) \in (0, \frac{2}{3}] \times (0, 1), \\ 20\pi^2 \sin 4\pi x \sin 2\pi y, & (x, y) \in (\frac{2}{3}, 1) \times (0, 1). \end{cases}$$

The exact solution is

$$u(x, y) = \begin{cases} \sin \pi x \sin 2\pi y, & (x, y) \in (0, \frac{2}{3}] \times (0, 1), \\ \sin 4\pi x \sin 2\pi y, & (x, y) \in (\frac{2}{3}, 1) \times (0, 1). \end{cases}$$

Since  $\kappa$  is discontinuous at  $x = 2/3$ , we use the randomly distorted mesh shown in Figure 5.3. Hence each cell is homogeneous, but material properties may vary between cells. We give the error between the exact solution and the numerical solution on a randomly distorted mesh in Table 5.3. From this table, we see that our scheme has nearly second-order convergence for this problem with discontinuous coefficients.

**6. Conclusion.** We present a new construction of vertex unknowns in the nine point scheme for discretizing diffusion operators on distorted quadrilateral meshes. The resulting scheme has only the cell-centered unknowns and has a local stencil; moreover, it treats material discontinuities rigorously and offers an explicit expression for the face-centered flux. Furthermore, the expression of the normal flux component has a specific physical meaning. In addition, we can obtain the vertex values. Our scheme is nonsymmetric in general and reduces to the standard five point scheme on rectangular grids. Although the construction of our scheme is described only on distorted quadrilateral meshes, it is straightforward to extend it to arbitrary polygonal meshes.

**Acknowledgments.** The authors thank the two reviewers for their numerous constructive comments and suggestions that helped to improve the paper significantly.

#### REFERENCES

- [1] I. AAVATSMARK, *An introduction to multipoint flux approximations for quadrilateral grids*, Comput. Geosci., 6 (2002), pp. 405–432.
- [2] I. AAVATSMARK, T. BARKVE, Ø. BØE, AND T. MANNSETH, *Discretization on unstructured grids for inhomogeneous, anisotropic media. Part I: Derivation of the methods*, SIAM J. Sci. Comput., 19 (1998), pp. 1700–1716.
- [3] I. AAVATSMARK, T. BARKVE, Ø. BØE, AND T. MANNSETH, *Discretization on unstructured grids for inhomogeneous, anisotropic media. Part II: Discussion and numerical results*, SIAM J. Sci. Comput., 19 (1998), pp. 1717–1736.
- [4] I. AAVATSMARK AND G. T. EIGESTAD, *Numerical convergence of the MPFA O-methods and U-method for general quadrilateral grids*, Int. J. Numer. Methods Fluids, 51 (2006), pp. 939–961.
- [5] B. ANDREIANOV, F. BOYER, AND F. HUBERT, *Discrete duality finite volume schemes for Leray-Lions type elliptic problems on general 2D meshes*, Numer. Methods Partial Differential Equations, 23 (2007), pp. 145–195.
- [6] K. DOMELEVO AND P. OMNES, *A finite volume method for the Laplace equation on almost arbitrary two-dimensional grids*, ESAIM Math. Model. Numer. Anal., 39 (2005), pp. 1203–1249.
- [7] F. HERMELINE, *A finite volume method for the approximation of diffusion operators on distorted meshes*, J. Comput. Phys., 160 (2000), pp. 481–499.
- [8] W. HUANG AND A. M. KAPPEN, *A Study of Cell-Center Finite Volume Methods for Diffusion Equations*, Mathematics Research Report 98-10-01, Department of Mathematics, University of Kansas, Lawrence KS, 1998.
- [9] D. S. KERSHAW, *Differencing of the diffusion equation in Lagrangian hydrodynamic codes*, J. Comput. Phys., 39 (1981), pp. 375–395.
- [10] D. LI, H. SHUI, AND M. TANG, *On the finite difference scheme of two-dimensional parabolic equation in a non-rectangular mesh*, J. Numer. Methods Comput. Appl., 4 (1980), pp. 217–224.
- [11] K. LIPNIKOV, M. SHASHKOV, AND D. SVYATSKIY, *The mimetic finite difference discretization of diffusion problem on unstructured polyhedral meshes*, J. Comput. Phys., 211 (2006), pp. 473–491.

- [12] J. E. MOREL, J. E. DENDY, M. L. HALL, AND S. W. WHITE, *A cell centered Lagrangian-mesh diffusion differencing scheme*, J. Comput. Phys., 103 (1992), pp. 286–299.
- [13] J. E. MOREL, R. M. ROBERTS, AND M. J. SHASHKOV, *A local support-operators diffusion discretization scheme for quadrilateral  $r$ - $z$  meshes*, J. Comput. Phys., 144 (1998), pp. 17–51.
- [14] Y. SAAD, *Iterative Method for Sparse Linear Systems*, PWS Publishing, New York, 1996.
- [15] M. SHASHKOV, *Conservative Finite-Difference Methods on General Grids*, CRC Press, Boca Raton, FL, 1996.
- [16] M. SHASHKOV AND S. STEINBERG, *Support-operator finite-difference algorithms for general elliptic problems*, J. Comput. Phys., 118 (1995), pp. 131–151.
- [17] J. WU, S. FU, AND L. SHEN, *A difference scheme with high resolution for the numerical solution of nonlinear diffusion equation*, J. Numer. Methods Comput. Appl., 24 (2003), pp. 116–128.
- [18] X. YE, *A new discontinuous finite volume method for elliptic problems*, SIAM J. Numer. Anal., 42 (2004), pp. 1062–1072.
- [19] G. YUAN AND Z. SHENG, *Analysis of accuracy of a finite volume scheme for diffusion equations on distorted meshes*, J. Comput. Phys., 224 (2007), pp. 1170–1189.